A model to estimate the lifetime of structures located in seismically active regions

Fernando Lopez-caballero, Claudia Aristizabal, Mauricio Sanchez-Silva

A model to estimate the lifetime of structures located in seismically active regions

F. Lopez-Caballero[a,*], C. Aristizábal[a], M. Sánchez-Silva[b]

[a] *Université Paris-Saclay, CentraleSupelec, CNRS, Laboratoire de Mécanique des Sols, Structures et Matériaux, 91190, Gif-sur-Yvette, France*
[b] *Universidad de los Andes, Dept. of Civil and Environmental Engineering, Bogota, Colombia*

Abstract

Understanding and modeling the evolution of structural systems throughout time, especially by considering its cumulative damage, is a key point for risk decision making. This concept is of extreme importance for design criteria definition, operational policies, robust life-cycle cost estimations and real time-dependent vulnerability assessment. In particular, an important objective of these type of analyses, is the estimation of the structure lifetime distribution and its corresponding mean time to failure (MTTF). However, analytic solutions of these two main concepts are not an easy task. Therefore, it is necessary to develop new approaches that can be used to better approximate the lifetime of structures in an accurate and useful way for engineering purposes. Within this context, the objective of this research work is to present a methodology to estimate the lifetime distribution of structures, and the derived properties of a structural system located in a seismic region.

*Corresponding author
Email address: fernando.lopez-caballero@centralesupelec.fr (F. Lopez-Caballero)

Mainshocks are modelled as a homogeneous Poisson process with constant mean rate of occurrence. The model, assumes that the deterioration of a given structure is mainly controlled by the cumulative damage generated by a set of consecutive earthquake events in a certain period of time. This approach can be easily implemented and provides a good estimation of the lifetime distribution of a structure, without venturing into the mathematical complexities of an analytic solution but retaining the main features of the system performance. Finally, an illustrative practical case at a real site is provided.

Keywords: Structure lifetime, Mean-Time-To-Failure, Earthquake, cumulative damage, shock-based degradation

1. Introduction

The Eurocode [1] defines the *design working life* of a structure as "... the period for which it [a structure] is to be used for its intended purpose with anticipated maintenance but without major repair being necessary." Similar definitions can be found in other standards such as the American Society for Civil Engineers (ASCE) [2]; and the British Standards BSI [3]. In engineering practice it is common to establish specific minimum structural lifetime values; for example, the Eurocode defines a design working life of 50 years for buildings and 100 years for bridges [1]. However, evidence has proven that infrastructure last longer, and some times far beyond than the values specified in technical standards. Arbitrary lifetime values set by design standards are, in practice, used as input to determine other important design parameters related mostly with the definition of the demand [1, 3, 4]. For instance,

heavy traffic on bridges or demands imposed by extreme events (e.g., seismic loading, hurricane gust winds). They are also used for considering material property deterioration, or as a reference to make life-cycle costing and define maintenance strategies. In summary, the structural lifetime is not explicitly set as a design objective *per-se*. This "unconscious" decision transfer the responsibility of maintaining and handling possible future failures to future generations.

Mathematically, the *lifetime* of a structure is the time that takes for a structural performance indicator to reach a predefined threshold, which separates acceptable from unacceptable behavior. Common performance indicators include, for example, the structural capacity or a reliability measure (e.g., reliability index β, deformation threshold). Thresholds are defined depending on the purpose of the structure and are usually referred to as *limit states*. Two limit states are of particular interest in engineering design: serviceability and ultimate limit states. Structures can reach these performance thresholds as a result of degradation processes, cumulative damage or due to the occurrence of sudden disproportionate large events (catastrophic event).

Since the structural performance and the occurrence of external events cannot be fully predicted; the processes leading to failure (i.e., surpassing a limit state) are highly uncertain. Thus, the structural lifetime, which is a random variable, X, needs to be characterized through a probability distribution, $F_X(t)$; where the expected value, $\mathbb{E}(X)$, is referred to as the Mean Time To failure (MTTF) and it is an important parameter for decision making. It is used to define important actions that go from the selection of inspection and intervention times to the abandonment or replacement of the

project [5, 6, 7].

In order to estimate the lifetime distribution of a structure, it is necessary to build a model capable of predicting the structural performance and cumulative damage over time. The structural performance depends on both external (e.g., environmental demands) and internal aspects (e.g., material degradation) and their relationship with the structural features. As stated by Ranjkesh et al. [8], most degradation models are either of the deterioration-based [e.g. 9, 10, 11] or the shock-based type [e.g. 12, 13]. The deterioration-based degrades due to internal factors such as ageing, overload, wear, or corrosion. The second type involves systems subjected to a sequence of shocks or external factors that can be modelled by a stochastic point process. The methodology proposed in this work is of shock-based type without the possibility of any type of repair during the degradation process.

For example, in high seismicity regions, the structural lifetime is mostly controlled by the damage accumulated as a result of earthquakes that occur randomly in a particular seismic area source or fault over a certain period of time. The effect of earthquakes can be modeled as shock-based deterioration process; i.e., events that cause sudden changes (damage) on the structural properties (described by any performance indicators) over time [7].

In the literature, several models have been developed to characterize the cumulative structural deterioration as a result of earthquake events [14, 15, 16, 17, 18, 19]. Modeling degradation, in general, has two main difficulties: (i) degradation is an unobservable (latent) process [20], which results from the complex combination of different mechanisms (e.g., fatigue, corrosion, etc.); and (ii) there is not enough data to characterize statistically the processes

and the variables involved. Furthermore, analytical models become highly complex very quickly and is difficult to find a close form solution [7]. The long-expected lifetime of structures and infrastructure, added to the complexities that involve modeling degradation, have put aside the problem of estimating the lifetime in practical design. Thus, in addition to the already existing mathematical tools [7], it is necessary to develop new approaches that can be used to approximate the structure's lifetime in a way that is useful in engineering practice. These tools might have an important impact in defining design criteria, operational policies, and making more robust life-cycle cost estimations.

The objective of this paper is to present a simplified and practical method to estimate the lifetime (and the MTTF) of structures located in active seismic regions using a shock-based degradation model. The model proposed here describes the process of damage accumulation as the structure is subjected to a sequence of earthquakes during a certain period of time; and allows computing the distribution and the MTTF without deepening into the mathematical complexities that are required for an analytical solution, but preserving the main features of the system performance. The lifetime distribution can be computed for various limit states, in accordance to the decision makers needs. The model presented in this paper does not take into account additional degradation mechanisms (e.g., fatigue, corrosion), nor any kind of retrofiring, but they can be further incorporated in the methodology if required. The earthquake recurrence model used follows a homogeneous Poisson process (HPP), nevertheless any other recurrence model, such as clusters, foreshocks and aftershocks can be easily used by modifying the syn-

thetic earthquake catalogue number of events and distribution in time, since the method is completely versatile with respect to the recurrence model and the type of structure. Finally, the proposed approach combines analytical models of the structure and the local seismic hazard.

This paper is structured as follows. First, it presents a definition of the structural lifetime and brief review of the shock-based degradation process; some of the most common models are mentioned and discussed. This discussion is used as the basis for justifying the proposed simplified model. Then, the basic assumptions and the step-by-step description of the approach is presented. Finally, in order to show the applicability and the results of the model, it is illustrated with a case study of a concrete structure located at the Euroseistes in Greece. As a result, the lifetime distributions for various limit states are shown and discussed.

2. Evaluation of the structural performance over time

2.1. Structural lifetime

Consider a structure that is placed in operation at time $t = 0$ and whose condition at time $t > 0$ is denoted by $V(t)$, which is a random variable that takes values in the set of positive real numbers. It is assumed that $V(0)$ is deterministic and represents the structural initial condition. Note that the random variable $V(t)$ characterizes the evolution in time of a specific performance indicator. Furthermore, let's define the random variable $X(t)$, with $X(0) = 0$ (almost surely), as the accumulated deterioration until time t; with $X(t)$ a continuous non-decreasing function in t. Then, under the assumption that there is no maintenance, or any other intervention that

modifies $V(t)$ before failure, the system condition at time t can be computed as [7]:

$$V(t) \;=\; \max\{V(0) - X(t), 0\} \tag{1}$$

Note that the sets $\{V(t)\}_{t\geq 0}$ and $\{X(t)\}_{t\geq 0}$, which consists of the random variables describing the condition and deterioration for all times $t \geq 0$, constitute stochastic processes with continuous state space and continuous time. System failure occurs when the condition of the system falls bellow a predefined threshold s^*, with $0 \leq s^* \leq V(0)$, that represents any serviceability, operational or ultimate limit. Then, the system lifetime L is also a random variable given by:

$$L = \inf\{t \geq 0 : V(t) \leq s^*\} \;=\; \inf\{t \geq 0 : X(t) \geq V(0) - s^*\}. \tag{2}$$

Two important quantities can be derived from the lifetime distribution: i) the mean time to failure (MTTF); and ii) the reliability function. The MTTF$= \mathbb{E}[L]$, where $\mathbb{E}[\cdot]$ is the expectation operator. Besides, the reliability is defined as the probability that the system accomplishes its intended function in a designated period of time t (e.g., at the system's mission time t_m). It is the probability that the condition $V(t)$ is greater than the threshold s^*; i.e.,

$$R(t) = P\left(V(t) \geq s^*\right) \;=\; P\left(X(t) \leq V(0) - s^*\right) \tag{3}$$

Therefore, if the derivative of $R(t)$ exists, the density function $f(t)$ of the lifetime is given by [7]:

$$f(t) = -\frac{d}{dt}R(t) \;=\; -\frac{d}{dt}P\left(X(t) \leq V(0) - s^*\right), \tag{4}$$

2.2. Structural degradation caused by shocks

Degradation models describe the damage accumulation in any system as a result of its dynamic interaction with external demands or internal changes of the structure. Frequently, degradation models are divided into two basic mechanisms: i) progressive degradation, in which the system condition (system properties) decreases continuously over the time (e.g., aging, wear or corrosion); and ii) shock-based degradation, where the system condition is subject to sudden changes (decays) at specific points in time (e.g., structures subjected to earthquakes or blasts) [21]. In this paper we will focus only on the latter; details of progressive degradation models can be found in Sánchez-Silva and Klutke [7].

Shock-based degradation models consider the cumulative effect of sudden (and independent) events that remove finite amounts of the system's capcity, in the form of jumps or shocks, at discrete points in time [22, 23, 21, 24]. Shock-based degradation can be described by two stochastic processes: i) the inter-arrival times $\{T_i\}_{i\geq 1}$ (with T_i the random variable of the time between the $(i-1)^{th}$ and i^{th} shock); and ii) shock sizes $\{Y_i\}_{i\geq 1}$, which represent the damage of each shock to the system. If after each shock damage accumulates and no maintenance is performed, the total deterioration by time t, $D(t)$, can be computed as:

$$D(t) \quad = \quad \sum_{i=1}^{N(t)} Y_i, \tag{5}$$

where $N(t)$ is a random variable describing the number of shocks by time t. Hence, the system's capacity by t can be expressed as:

$$V(t) = V(0) - D(t) \quad = \quad V(0) - \sum\nolimits_{i=1}^{N(t)} Y_i, \tag{6}$$

and the reliability function becomes:

$$R(t, s^*) = \mathrm{P}(D(t) < s^*) \quad = \quad \mathrm{P}\left(\sum_{i=1}^{N(t)} Y_i < s^*\right) \tag{7}$$

When computing the reliability function, it is important to distinguish between two cases: i) models where degradation caused by one shock depends on the history of the process up to that point; and ii) those where the shock damages accumulates in an independent manner. The proposed model is based on the second assumption, which is evaluated indirectly through simulations. The discussion on the details of these models is beyond the scope of this paper but can be found, for instance, in Sánchez-Silva and Klutke [7].

An analytical solution to compute the reliability and the lifetime distribution, involves the evaluation of the distribution of the sum of n random variables (i.e., shock sizes and inter-arrival times), which requires the evaluation of n-fold convolutions, and to take the limit $n \to \infty$. In general this is a difficult problem and, with few exceptions, Monte Carlo simulation is the only option to obtain a solution. Among the analytical solutions, the most common models are the compound Poisson Process (CPP) [7], and the use of Phase-type distributions [19].

3. Simplified methodology for lifetime estimation

3.1. Basic assumptions

The model is based on the following assumptions:

- All ground motions included in the analysis (i.e., actual or simulated) keep the basic seismic characteristics (i.e., magnitude range, distance

range, site amplification, spacial distribution, among others) than those recorded in the area where the structure is located.

- The structural performance is characterized by performing non-linear dynamic analyses of a structural model under a suite of ground motion records. The used numerical model allows to take into account a state-dependent seismic response, or in other words, the damage caused by previous earthquakes.

- The damage caused by an earthquake event, i.e. the engineering demand parameter (EDP), could be quantified in buildings with both peak and residual lateral inter-story drift demands. In this work for the sake of simplicity the cumulated induced maximum top displacement will be used. Nevertheless any other damage indicators are also suitable to be used under the proposed methodology [e.g 25, 26, 27, among others].

- The structure is not intervened (e.g., retrofitted) after it has experience a ground motion.

The proposed model is highly flexible and can be adapted to the specific conditions of the problem at hand. In the first assumption (i.e., selection of seismic records) the main restriction is that the seismic nature of the events selected should resemble as much as possible the seismicity of the area. In the third assumption, other structural performance models and damage measures can be implemented if needed. The last restriction cannot be modified because it will change the way in which the lifetime is estimated.

3.2. Overall description of the model

A conceptual flow diagram of the method is presented in Figure 1. Consider a well known structural system located in an area whose seismic activity is well documented and characterized (i.e., magnitude of events M_w, recurrence, duration, peak ground acceleration, frequency content, etc.). Based on existing seismic information, K trains of N earthquake records are constructed. The selection of events and their order of occurrence are selected based on a previous statistical characterization and considering the local recurrence model at the site of interest. The structure is then subjected to every train of events until it exceeds a damage state (i.e., failure); or it has been subjected to all N events in the train (no failure). Then, after subjecting the structure to a large number of earthquake trains, the probability of reaching a particular damage state can be computed; and since the occurrence rate of earthquake events is known, the time to failure can be easily evaluated as well. The details of the process is presented in the following sections.

3.3. Seismic hazard characterization

The first step consists of determining the seismicity of the site in which the building is located or where it will be built. The three main aspects to be determined are: i) the geographical location of the building; ii) the site characteristics (i.e., soil class, the average shear-wave velocity (V_s) for the upper 30 m depth ($V_{S,30}$), among others); and iii) the magnitude-frequency distribution and the special distribution of earthquakes. Once the previous aspects are defined, there are two types of methods to perform seismic risk

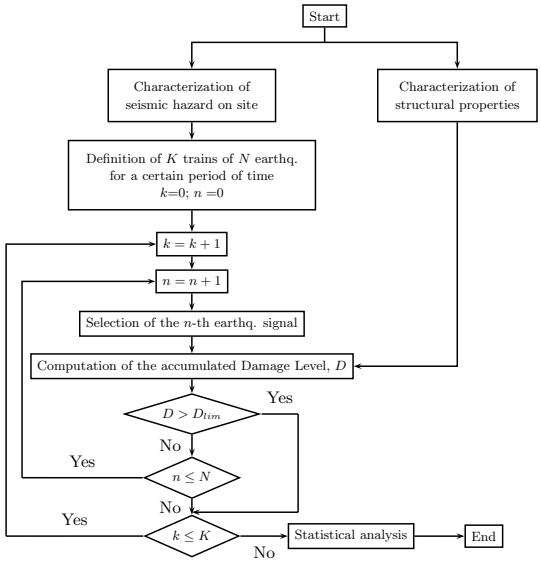

Figure 1: Flow diagram of the simplified method to estimate the lifetime of structures in earthquake prone areas.

assessment: Non-site-specific and site-specific approaches. The former considers multiple time histories from multiple sites, while the later uses only site-specific time histories based on on local parameters, local recurrence of earthquakes (or number of expected earthquakes at a given period of time). Now, if sufficient amount of data is available at the site, site-specific approaches better estimate the local seismic hazard and its local variability, hence, a better estimation of the cumulative damage will be retrieve. Nevertheless, it is often common a lack of local data at the site of interest, then, a non-site specific approach might be required.

Once the main aspects that characterize the local seismic hazard are defined, it is possible to proceed with the selection of time history. Two main strategies for this purpose can be used: i) Spectral matching using

real accelerograms; or ii) stochastic time histories generation using local site conditions. Even though both methods should be applied considering both local magnitude-distance disaggregation and magnitude-frequency distribution (better known as truncated Gutenberg-Richter model) at the site of interest, the later will also required extra information for the source, path and site synthetic models (e.g., stress drop distribution, S and P waves velocity profiles, high frequency attenuation factor (κ), among others, see Aristizábal et al. [28] for further information).

There exist also two ways of generating the accelerograms: i) compatible to the uniform hazard spectrum (UHS), or ii) compatible to the design spectra of a given seismic design code. For case i), the authors believe that the selection of accelerograms should be done based on the UHS rather than on design spectra. The reason for this preference choice, is because even though both are envelops of the local hazard, the UHS provides the same probability of exceeding a certain ground motion level at a given site for different spectral periods, while the design spectra is just a simplified and truncated way of representing the variability of the local response spectra at different sites for a given site class and for different spectral periods. The accelerograms can be fitted to a rock or a soil spectra, if the former is used, then a soil transfer function needs to be apply to consider for local soil conditions. On the other hand, concerning the stochastic time histories using local site conditions, there exist several different methods to generate the synthetic waveforms [29, 30, 31, 32, among others] where the magnitude and distance ranges can be predefined.

3.4. Definition of ground motions sequences

During the structure's lifetime, damage accumulates as a result of a sequence of events that are distributed over time. Let's assume that $S = \{S_{t_1}, S_{t_2}, ...S_{t_n}\}$ is a set of n events that occur at times t_i in a sequential manner i.e., $t_{i-1} < t_i$. Then, the total damage, $D(z)$, after the z-th event will be:

$$D(z) = \sum_{i=0}^{z} \Delta D(\Delta\delta_{M_i}) \tag{8}$$

where $\Delta\delta_{M_i} = \delta_{M_i} - \delta_{M_{i-1}}$. The term $\Delta\delta_{M_i}$ represents the change in the maximum response deformation at the i-th seismic excitation only; with $\delta_{M_0} = 0$. However, trains of ground motions can be organized in many different ways; i.e., they can occur in different order. Therefore, the damage accumulated after the z-th event depends on the order in which the events were selected. Let's define the j-th random sequence as S_j, then, the probability that the damage exceeds a threshold s^* in the z-th earthquake event can be computed using Monte Carlo Simulation.

$$\mathbb{P}(D(z) > s^* | D(z-1) \leq s^*) = \frac{\text{Number of cases with } D(z) > s^*}{k_z} \tag{9}$$

where k_z is the number of sequences S in which the system has not failed at the z-th event. The number of events required for the structure to reach the threshold s^* varies; however, there might be earthquake sequences where the threshold is achieved only after a large number of events. In these cases, the probability evaluation made using equation 9 may not converge (even for an extremely large number of simulations). This can be observed when

plotting equation 9 vs z (see section 4). Thus, in order to ensure consistency in the assessment, the number of events in a sequence should be limited; for instance, setting a boundary on the difference between the probability of failure of event z and event $z-1$.

This model considers the realistic case in which degradation caused by one shock depends on the history of the process up to that point (see section 2.2); i.e., the shock size distribution of one event depends on the accumulated damage just before the event occurs. Increasing damage with time, conditioned on the history of the process, can be model, for instance, as [7]:

$$X(t) = \sum_{i=1}^{N(t)} g(Y_i, V(t_i^-)) \tag{10}$$

where Y_i is the i-th shock size, $V(t_i^-)$ is the structural condition just before the i-th event, $N(t)$ is a random variable describing the number of events by time t, and $g(Y_i, V(t_i^-))$ is a continous function nonincreasing in V and non-decreasing in Y. Nevertheless, this path-dependency is difficult to capture in practice, mainly because there is not enough historical data. This probability is also difficult to evaluate analytically since it involves the computation of convolutions (sum of shock size distribution).

However, the probability distribution describing the history of the process, $G(y, z)$, where y is the damage level and z the number of the event in the sequence, can be captured in equation 9. Then, let's assume that the damage exceedence probability distribution at any event z has the same general form, but different parameters $\Phi = \{\phi_1(z), \phi_2(z), ..., \phi_w(z)\}$; e.g., lognormal with varying mean $\mu(z)$ and variance $\sigma(z)$. Note that the distribution does not

depend on time but on the position in the sequence. If damage is assumed to be a monotonic increasing function, regression analysis can be used to estimate every parameter $\phi_i(z)$; and, consequently, it is possible to obtain a full description of $G(y, z)$. This result is important because it allows to estimate the distribution that characterize the probability that the damage exceeds a given threshold s^*, after a given number of earthquake events z in a specific seismic environment. Furthermore it captures, at least in an approximate manner, the inherent dependence of the process (i.e., accumulated damage) on the damage observed at the z-th event.

3.5. Time variant assessment of failure probability

In order to compute the lifetime distribution, it is necessary to take into account the times at which events occur. Then, note that equation 5 can be used to compute the total damage after $N(t)$ events; with $N(t)$ a time-dependent random variable. If the event $z-1$ occurs and the accumulated damage does not exceed the threshold s^*, the probability that this threshold is surpassed in the next earthquake event (i.e., z) is computed as:

$$\mathbb{P}(D(z) > s^* | D(z-1) \leq s^*) \quad = \quad \int_{s^*}^{\infty} dG(y, z, \Phi_z) \tag{11}$$

where Φ_z is a vector with the parameters of the distribution G at the z-the event. If the system is exposed to successive shocks until it fails, and then abandoned (i.e., the system is not reconstructed or intervened in any way after failure), the system may reach the threshold s^* in the first event, or the second, or after a large number of events. Then, the probability of failure is conditioned on the number of events in a given time t, i.e.,

$$\mathbb{P}(D > s^*, t) \;=\; \sum_{z=1}^{\infty} \left(\int_{s^*}^{\infty} dG(y, z, \Phi_z) \right) \mathbb{P}(N(t) = z, t) \qquad (12)$$

where

$$\mathbb{P}(N(t) = z, t) \;=\; \frac{(\lambda t)^z}{z!} \exp(-\lambda t) \qquad (13)$$

where λ is the occurrence rate of earthquake events and $\mathbb{P}(N(t) = z, t)$ is the probability of having z shocks by time t; note that it removes the condition on z. Equation 12 describes the probability of failure at a given time t, which describes its time-variant nature. A significant contribution of this approach is that in Equation 12 it is not necessary to compute the convolution of shock size distributions, making the evaluation more efficient computationally.

4. Illustrative example

4.1. Structural model

The reinforced concrete building chosen for the study was the one proposed by Marante et al. [33], Sáez et al. [34]. It is a large-scale, one-span, two-story frame model. The total structure height is 4.2 m and the width is 4.0 m (Figure 2a). The dimensions of transverse sections are 0.4 m × 0.3 m for the beams and 0.4 m × 0.4 m for the columns. The mass of the building is assumed to be uniformly distributed along beam elements and the columns are supposed massless. The total mass of the building is 40 T. With these characteristics the fundamental period of the structure (T_{str}) is equal to 0.24 s. In order to simulate the nonlinear material response of the structure, beam-column elements with plastic hinges were used. The model

is based on the two-component model presented by Giberson [35] and the modifications introduced by Prakash et al. [36] to take into account axial force (P) and bending moment (M) interaction by specifying $P - M$ yield surfaces (Figure 2b). Refer to Prakash et al. [36], Sáez et al. [34] for further details about the model. All computations were conducted with GEFDyn Finite Element code [37].

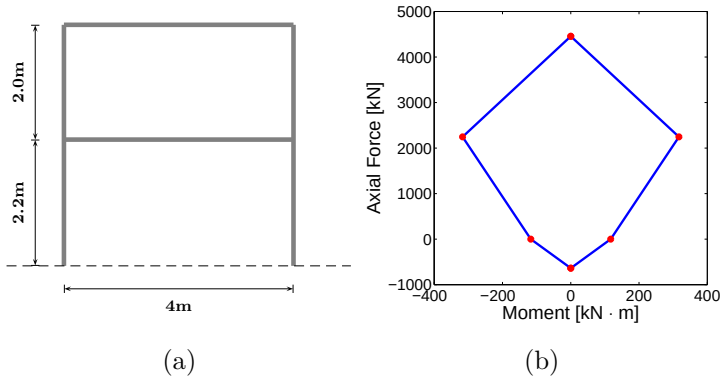

(a) (b)

Figure 2: a) Building geometry and b) Axial force-moment interaction diagram used for plastic-hinge column elements of the building [34].

Let's consider that this building is located in the Euroseistest site in Greece on a hard rock site, a well-known experimental site for integrated studies in earthquake engineering [38]. The objective of this example is to obtain the lifetime distribution of the structure for various damaging limit states.

First of all, the dynamic response of the building model in a fixed base condition was analyzed using the whole sets of signals independently, i.e. without a specific sequence. The seismic demand on the building, namely, the maximum top displacement (u_{top}) and its corresponding shear strength

(V) are shown in Figure 3. In the same figure, the corresponding capacity curve obtained by a pushover test is also plotted.

The limit damage states (performance thresholds) adopted were those proposed by Penna et al. [39] and Del Gaudio et al. [40]; they are summarized in Table 1. Note that in Figure 3, only for some few signals a structural non-linear behaviour appears (i.e. $u_{top} > \Delta_y$, where Δ_y is the displacement corresponding to the yield capacity of structure). If μ is defined as the ductility ratio ($\mu = u_{top}/\Delta_y$, with $\Delta_y = 1.06$ cm from pushover test), in this case the ductility ratio varies from 1 to 1.35. This ductility ratio corresponds to the one obtained for the maximum u_{top} value.

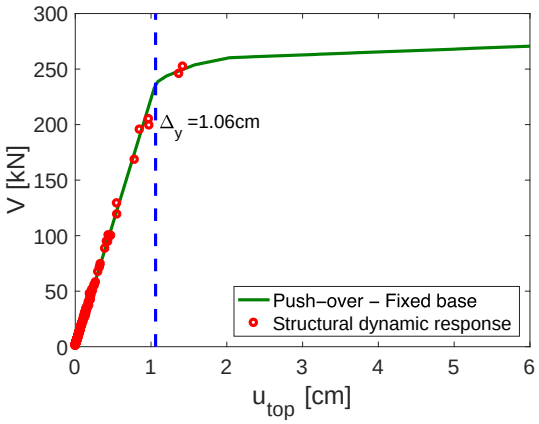

Figure 3: Structural dynamic response obtained for the building at fixed base condition compared with the static capacity curve.

4.2. Seismic hazard characterization

The next step in the process is the definition of: i) the cumulated damage of a structure; ii) its probability of failure due to different series of seismic shocks and iii) its associated uncertainty related to the order of earthquake occurrence (the Stochastic Earthquake Catalogue, SEC), as proposed

Table 1: Displacement limit states adopted in the illustrative example

Damage state	Displacement threshold	Displacement value* [cm]	Inter-story Drift Ratio (IDR)** [%]
Slight	$0.7 \cdot \Delta_y$	0.74	0.08
Moderate	Δ_y	1.06	0.32
Extensive	$\Delta_y + 0.25 \cdot (\Delta_u - \Delta_y)$	2.30	0.94
Complete	Δ_u	6.00	1.78

* Values used in the illustrative example [39]

** Values from Del Gaudio et al. [40]

by Aristizábal et al. [28] was used. The following stages were performed to obtain different series of seismic shocks:

- The catalogue of ground motions was constructed by sampling events from the European SHARE model [41] enclosing the Euroseistest site in Greece (GRA390). The magnitude-frequency distribution is shown in Figure 4a.

- In order to generate stochastic ground motion time histories, the stochastic method proposed by Boore [42] was used. This procedure is explained in Aristizábal et al. [28]. This method is implemented using the SMSIM code [43]. Nevertheless, any other suitable method for this purpose could be used.

- The SEC was built for seismic records on hard rock (V_s=2600 m/s) at site; the hazard curve built from this catalogue is shown in Figure 4b.

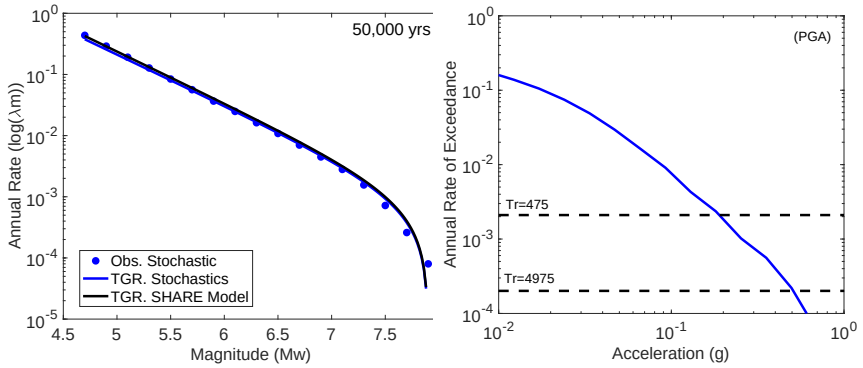

(a) (b)

Figure 4: a) Truncated Gutenberg-Richter recurrence models of the 50,000 years catalogue lengths compared with the original recurrence model of the source zone GRAS390 in the SHARE model and b) Hazard curves for PGA spectral periods built from the SMSIM stochastic time histories. (Figures from Aristizábal et al. [28]).

It is created from a 50,000 year stochastic earthquakes catalogue with $\approx$ 21,800 events ranging from magnitudes M_w = [4.5 to 7.8], Joyner and Boore distances [44] from RJB = [0 to 150] km and a hypocentral depth from D_{hyp} =[0 to 30] km. The probability density function (PDF) of the ground motion acceleration (PGA) on hard rock for different magnitude and distance ranges of the SEC is shown in Figure 5.

- Then, from the catalogue 21 different sub-catalogues of 100 years were randomly sampled; they correspond to 44 acceleration time histories in each sub-catalogue. Finally, to account for the randomness of shock sequences (i.e., order of occurrences), the 44 events in each sub-catalogue were permuted randomly; this procedure is repeated 15 times for each sub-catalogue. This resulted in the final sample of 315 sub-sets to be

used for each computation of 44 seismic shock sequences. The same procedure was done for the 21 different sub-catalogues of 50 and 75 years which contain 22 and 33 acceleration time histories each one respectively.

This work is based on a classical poissonian PSHA Guttenberg-Richter recurrence models extracted from the European SHARE model [41], since

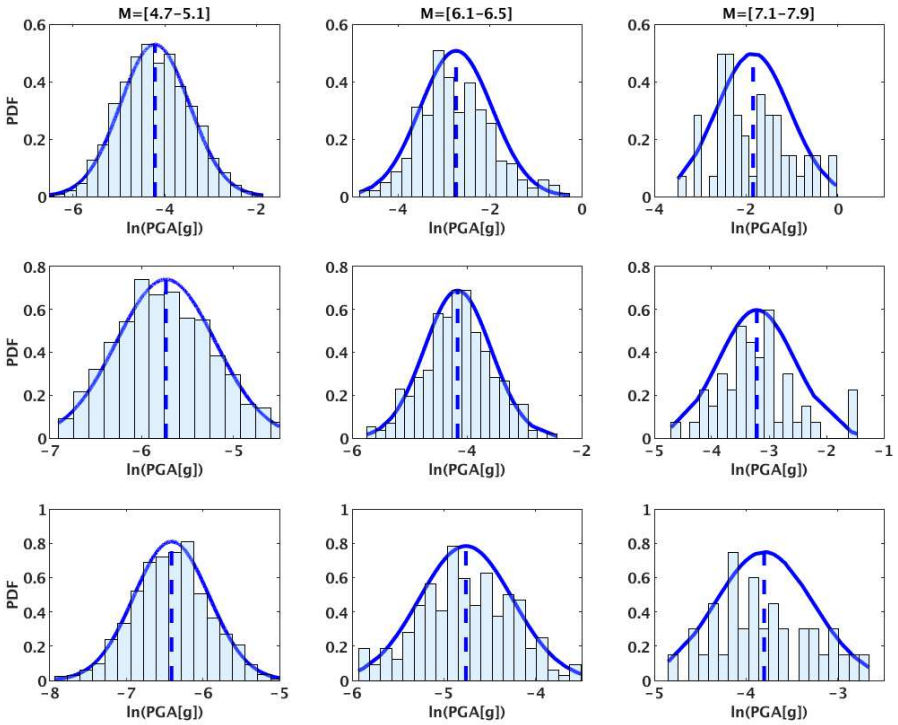

Figure 5: Probability density function (PDF) of the ground motion acceleration (PGA) on hard rock for different magnitude and distance ranges of the SEC. The Joyner and Boore distances R_{JB} from [0 to 150] km and a hypocentral depth D_{hyp} from [0 to 30] km. (Figures from Aristizábal et al. [28]).

this is the methodology that is widely used in earthquake engineering to derived earthquake recurrence models and the majority of seismic hazard maps worldwide. Under this assumption, the main shocks are assumed to be independent, hence aftershocks and foreshocks are discarded and removed from the catalogue. Nevertheless, in some specific cases to better estimate the real lifetime of a structure, it is important to add clusters as suggested by several authors [e.g. 45, 46, 47, 48, 49, 50, 51, 52]. But this issue is not addressed in this publication, since the aim here is to present the methodology and to show its versatility to better estimate the real lifetime of a structure subject to cumulative damage.

If it is necessary to consider the additional effect of such clusters, it will need only to add the foreshocks and aftershocks before and after each main shock of the synthetic earthquake catalogue and run again the FEM calculations considering the cluster for each main shock. The methodology presented here is so robust, that it can easily be used with any type of recurrence model (including or not aftershocks and foreshocks) that the user considers "realistic" for any case example than the one presented in this article.

4.3. Structural performance when subjected to trains of earthquakes

In order to compute the lifetime distribution it is necessary to model the structural performance when exposed to multiple sequences of ground motions. This means, evaluating the accumulated damage in a sequence of events until the total damage reaches a defined damage threshold; i.e., $u_{top} \geq u_{lim}$; where u_{top} is the maximum roof displacement and u_{lim} the limit state under consideration or $IDR \geq IDR_{lim}$ (see Table 1). Figure 6a shows u_{top} values for 315 trains of earthquakes with a time window of 100 years; i.e.,

every mark indicates the u_{top} for structure after 1,2,3,...44 ground motions. Two limit states, defined according to Table 1, are also indicated with dashed lines; i.e. *Slight* damage: $u_{lim} = 0.74$; and *Moderate* damage: $u_{lim} = 1.06$ cm. In a similar way, Figure 6b displays the evolution of obtained IDR values for the same time window. In this case the two limit state are the ones proposed by Del Gaudio et al. [40] (i.e. 0.08% and 0.32%).

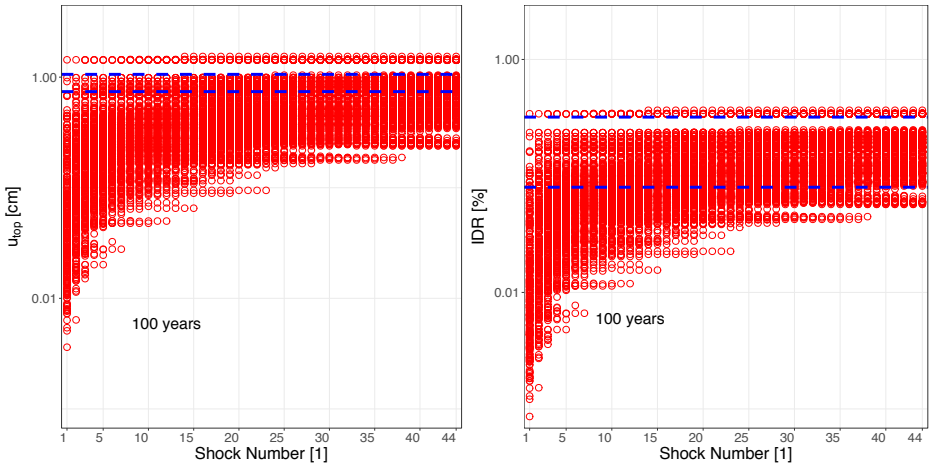

(a) (b)

Figure 6: Evolution of a) the u_{top} and b) the IDR, against the number of seismic shocks, for 44 earthquake trains, a period of 100 years.

In addition, Figure 7 displays the box plots of the obtained u_{top} (Figure 6a) and IDR (Figure 6b) evolution as a function of the number of seismic shocks for 100 years time windows. It is important to observe that as expected, the median of two variables, u_{top} and IDR increases as the number of seismic events in the sequence.

After N simulations (i.e., trains of events), there are N measurements of u_{top} and IDR for every position z in the sequence. These values represent

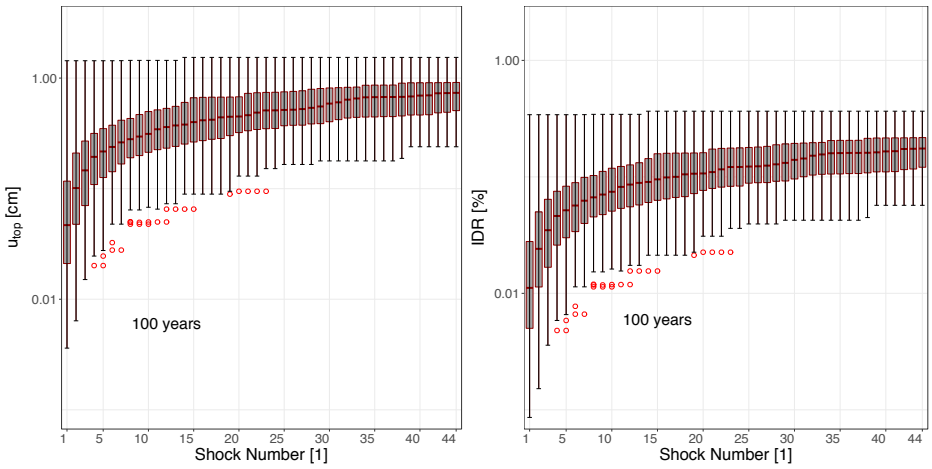

(a) (b)

Figure 7: Box plots of the obtained a) u_{top} and b) IDR, against the number of seismic shocks, for a period of 100 years.

possible damage states after the structure has been subjected to z ground motions. Then, the probability distribution of the total damage (i.e., u_{top} or IDR), $G(y, z)$, can be computed for every z. For example, for the problem at hand, and $z = 25$, obtained data from u_{top} can be adjusted to a logistic distribution with parameters $\mu = 0.561$ and $\sigma = 0.306$. Although it is not necessary, it is highly convenient to adjust $G(y, z)$ to the same functional form (e.g., logistic, lognormal); however, if this is not possible, the range of z values can be divided in sectors, where each one has the same functional form.

In this example, the analysis showed that in most of the cases, the logistic distribution fitted very well the data. Then, the logistic distribution was selected as the base damage distribution $G(y, z)$. The fittings for the mean

and standard deviation could be described with the equation 14.

$$G(y,z) \quad = \quad \beta_0 + \beta_1 \cdot z^2 + \beta_2 \cdot \ln(z) \tag{14}$$

Table 2 summarizes the obtained parameter values for the equation describing the evolution of mean and standard deviation of both u_{top} and IDR (Figure 8). In the Figure 8a, the *Slight* limit damage states for both u_{top} and IDR, are also plotted with dashed lines. It is important to note that in both cases, for lower shock number the mean value is lower than the damage limit, however, with the accumulation of shocks those limits are exceeded.

Table 2: Parameters for the estimated mean and standard deviation values of u_{top} and IDR as a function of z (equation 14).

	u_{top} [cm]			IDR [%]		
	β_0	β_1	β_2	β_0	β_1	β_2
$\hat{\mu}(z)$	0.0578	$9.226 \cdot 10^{-5}$	0.1468	0.0138	$2.190 \cdot 10^{-5}$	0.035
$\hat{\sigma}(z)$	0.168	$1.264 \cdot 10^{-5}$	0.0424	0.0364	$8.469 \cdot 10^{-7}$	0.0119

For illustrative purposes, the Empirical Complementary Cumulative Distribution Function (CCDF) of the u_{top} and IDR values, for various values of z, are shown in Figure 9. In the same figure, two limit damage states are also plotted with dashed lines; i.e. *Slight* damage and *Moderate* damage. From the results of this Figure, it is noted that the CCDF form will evolve with the increasing of the shock number. It may also be concluded that , in both cases, for the same level of damage state, the probability of exceedance is greater while the number of shock increases. It is also indicated that this

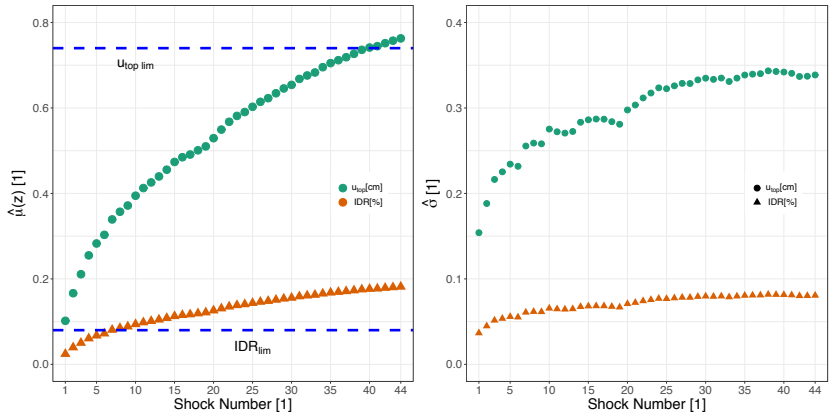

(a) (b)

Figure 8: a) Mean and b) Standard deviation evolution for every position z in the sequence of both u_{top} and IDR.

particular structure would be more prone to develop *Slight* damages than *Moderate* ones.

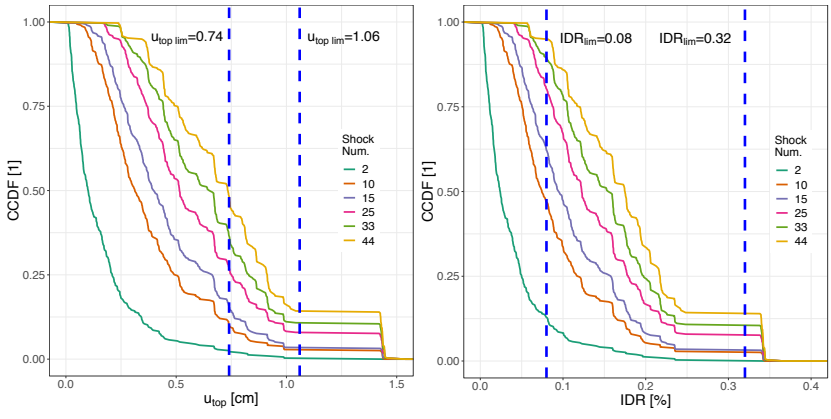

(a) (b)

Figure 9: Empirical Complementary Cumulative Distribution Function (CCDF) of a) u_{top} and b) IDR, for some z-th events.

4.4. Structural lifetime distribution

Now the lifetime distribution can be computed for various limit states and several performance indicators. Figure 10 shows the probability that the system's damage reaches a value larger than a threshold $s^* = u_{lim}$ or $s^* = IDR_{lim}$, as function of the number of shocks in a sequence; it is computed based on equation 9. For example, the probability that after 22 shocks the accumulated damage (u_{top}) is larger than 0.74 cm is about 25% and 75% for the case of IDR exceeds 0.08%. It is important to stress that the probability of exceedence starts fluctuating as the number of events to reach the failure increases. This is caused mainly by the fact that only in few cases the structure survive so many earthquakes. Therefore, the analysis was limited to a maximum number of shocks so that $\mathbb{P}(u_{top} > u_{lim}, z) - \mathbb{P}(u_{top} > u_{lim}, z - 1) \leq \zeta$, with z the number of shocks and ζ a predefined small value. In this example, the train of events was limited to 44 ground motions for 100-year time window.

In addition, it is well known that the choice of time window and consequently the size of the seismic shock sequences are key issues on the quality of the lifetime predictions. Thus, in order to study the evolution of the estimated probability to reach a damage state as a function of the size of the seismic shock sequences, the sub-catalogues for 50 and 75 years time windows were used. Figure 11 shows the probability that the system's damage reaches a value larger than a threshold $s^* = u_{lim}$ or $s^* = IDR_{lim}$, as function of both the number of shocks in a sequence and the time window. It can be observed that the response changes depending upon the damage level selected. Then, for $IDR_{lim} = 0.08\%$, the variation of the $\mathbb{P}(IDR \geq IDR_{lim})$ with respect to

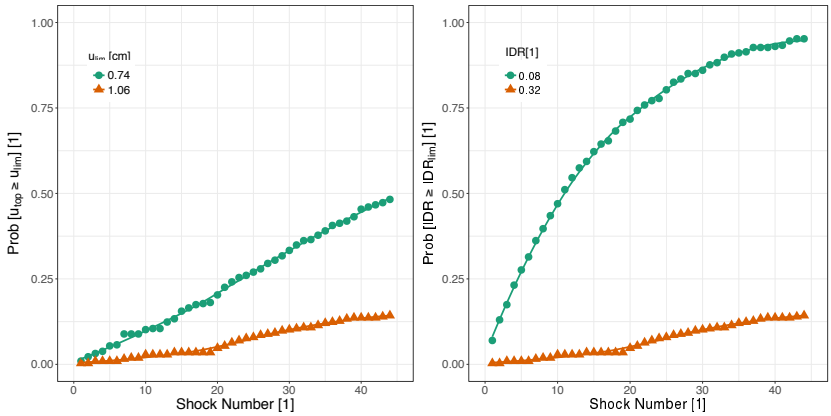

Figure 10: a) $\mathbb{P}(u_{top} \geq u_{lim})$ and b) $\mathbb{P}(IDR \geq IDR_{lim})$, for each seismic shock.

the time window is very small. However, for all other cases a bigger dispersion was observed. This dispersion is a function of the information provided by the size of the motion database (i.e. sub-catalogues) over the parameters describing the probability of failure (equation 9).

4.5. Lifetime distribution and Mean-Time-To-Failure

The occurrence rate of events was obtained for the studied case. There were 44 events, with the specifications defined for this study, therefore, $\lambda = 0.44$ earthquakes/year. Then, assuming that their occurrence follows a Poisson Process, the probability distribution of the time to failure can be easily computed using equation 12. The results are shown in Figure 12. For the studied building, it is noted that for the design working life of 50 years, the probability to exceed the *Slight* limit damage states is 24% and 75% for both u_{top} and IDR respectively. Concerning the *Moderate* limit damage states, the probability is close to 5% for both demand parameters.

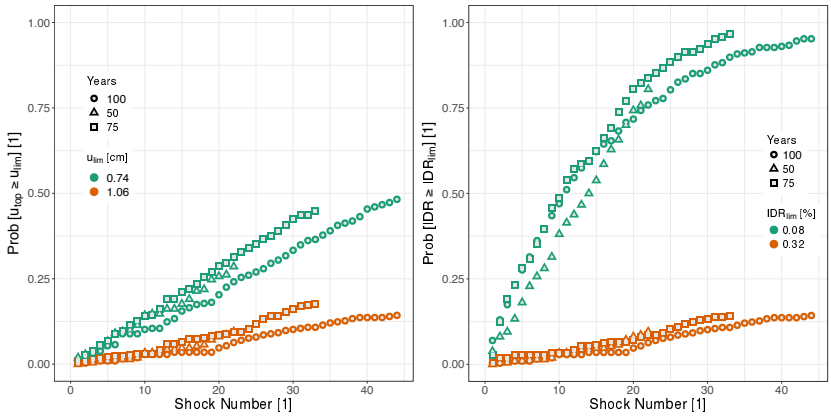

(a) (b)

Figure 11: Effect of the time window on a) $\mathbb{P}(u_{top} \geq u_{lim})$ and b) $\mathbb{P}(IDR \geq IDR_{lim})$, for each seismic shock.

507 Those probability values are above the requirements specified in the code of
508 practice.

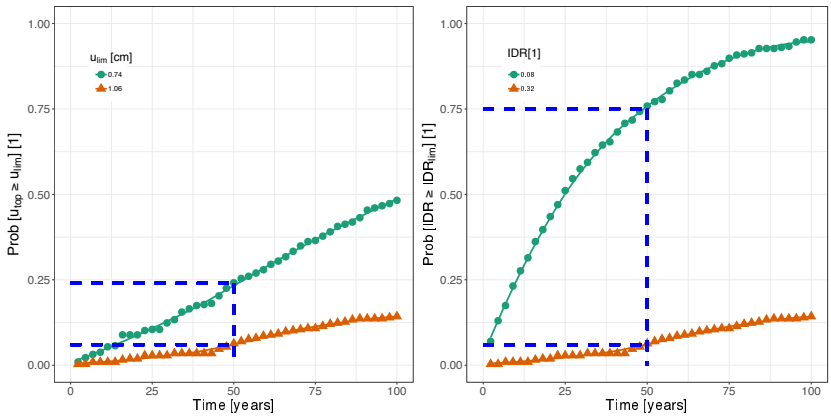

(a) (b)

Figure 12: a) $\mathbb{P}(u_{top} \geq u_{lim})$ and b) $\mathbb{P}(IDR \geq IDR_{lim})$, evolution with time.

509 Finally, so as to assess the failure time or survival time of the studied

structure, a survival analysis was used. This analysis gives the probability that the structure will survive past time t (i.e. the obtained demand parameter values are lower than the defined limit damage state). In this work the non-parametric Kaplan-Meier estimator [53] was employed for estimating the survival functions from observed survival times. In this method, it is assumed that the structure failure at each event occur independently of one another. Thus, the probability of not having a damage at time t_i, $S(t_i)$, is calculated by :

$$S(t_i) = S(t_{i-1})\left(1 - \frac{d_i}{n_i}\right) \tag{15}$$

where $S(t_{i-1})$ is the probability of not having a damage at t_{i-1}, n_j the number of case not having a damage just beforet_i and d_i the number of observed damages at t_i. At time $t = 0$, $S(t) = 1$.

Figure 13 displays the obtained survival curves for the *Slight* and *Moderate* limit damage states. The 95% confidence limits of the survivor function are also shown. It is noted that median survival time (MTTF) for the *Slight* limit damage states is 100 and 25 years for both u_{top} and IDR respectively (Figure 13a). For the IDR case the time-to-event curve follows a Weibull distribution ($S(t) = \exp(-\alpha \cdot t^{\gamma})$) with $\gamma = 1.119$ and $\alpha = 17.8 \cdot 10^{-3}$. Concerning the u_{top} case, the parameters are $\gamma = 1.285$ and $\alpha = 1.77 \cdot 10^{-3}$. Nevertheless, no information could be obtained from the survival curves for the *Moderate* limit damage states due to lack of observations (Figure 13b).

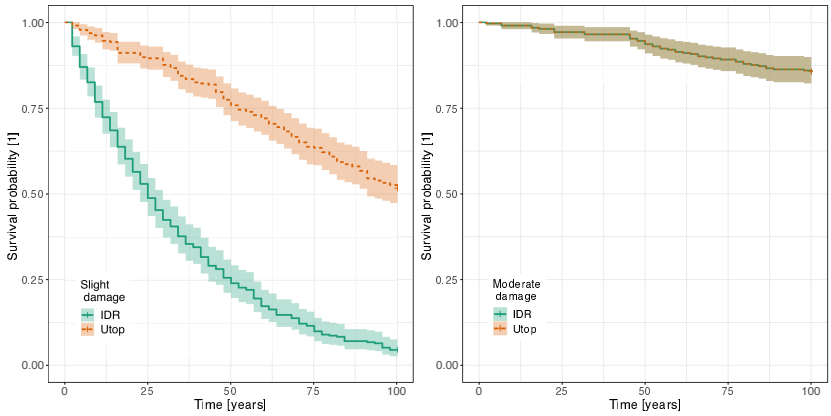

(a) (b)

Figure 13: Cumulative survival plots by a) *Slight* and b) *Moderate* limit damage states, evolution with time.

5. Conclusion

This paper presents a simplified model that can be used to estimate the lifetime distribution and the corresponding mean time to failure (MTTF) of a structural system located in a active seismic region. The model is intended to bring into practice the possibility of estimating the lifetime of a structural system without entering into the mathematical complexities that are required for an analytical solution, but retaining the main features of the evaluation. The model assumes that the structural deterioration is mainly controlled by the consequences of earthquake main shocks events. Then, it takes into account the accumulation of damage when the structure is subjected to a sequence of main shocks that occur randomly in time following a homogeneous Poisson process with constant mean rate of occurrence. The model allows estimating the lifetime for several performance limit states, which are

evaluated using the damage levels proposed in the literature, nevertheless any other damage indicators are also suitable to be used under the proposed methodology. The model has been developed so that it takes into account important aspects of the degradation process, the associated uncertainties and the actual modeling requirements. However, it makes some reasonable simplifications that overcome the complexities of analytical computations. Also, it uses an efficient simulation process that reduces the computational costs that imply a numerical, and sometimes in-existent, solution of the problem. Some aspects of the model can be refined or modify when required to capture specific characteristics of the seismic environment or the structure. Time span, damage indexes, recurrence models, type of structure, dynamic model, among others, can be modified easily together with its corresponding uncertainties using this method. Finally, the proposed model can be also used as evidence to make better decisions regarding operational policies, maintenance or life-cycle cost estimations.

Acknowledgements

A part of the research reported in this paper has been supported by the SEISM Paris Saclay Research Institute (www.institut-seism.fr/en/).

References

[1] Committee European de Normalization 250, Eurocode 1 - actions on structures part 1 - basis of design, European Pre-standard ENV 1991-1, Brussels (Belgium), 1994.

[2] American Society for Civil Engineers (ASCE), Minimum design loads for buildings and other structures; Standards ASCE/SEI 7-10, ASCE, Reston, VA, 2013.

[3] BSI, Structural use of steelwork in buildings part 1: Code of practice for design-rolled and welded sections, British Standards Institution, BS5950-1, Brussels (Belgium), 2000.

[4] SEI/ASCE 7-02, Minimum design loads for buildings and other structures, American Society of Civil Engineers, Reston VA, USA, 2002.

[5] C. Santander, M. Sánchez-Silva, Design and maintenance programme optimization for large infrastructure systems, Structures & Infrastructure Engineering 4 (4) (2008) 297–309.

[6] M. Sanchez-Silva, G. A. Klutke, D. V. Rosowsky, Life-cycle performance of structures subject to multiple deterioration mechanisms, Structural safety 33 (2011) 206–217.

[7] M. Sánchez-Silva, G.-A. Klutke, Reliability and LIfe-Cycle Analysis of Deteriorating systems, Springer, London, 2016.

[8] S. H. Ranjkesh, A. Z. Hamadani, S. Mahmoodi, A new cumulative shock model with damage and inter-arrival time dependency, Reliability Engineering & System Safety 192 (2019) 106047.

[9] D. M. Frangopol, K.-Y. Lin, A. C. Estes, Life-Cycle Cost Design of Deteriorating Structures, Journal of Structural Engineering 123 (10) (1997) 1390–1401.

[10] M. Akiyama, D. Frangopol, I. Yoshida, Time-dependent reliability analysis of existing RC structures in a marine environment using hazard associated with airborne chlorides, Engineering Structures 32 (11) (2010) 3768–3779.

[11] M. Akiyama, D. M. Frangopol, H. Matsuzaki, Life-cycle reliability of RC bridge piers under seismic and airborne chloride hazards, Earthquake Engineering & Structural Dynamics 40 (15) (2011) 1671–1687.

[12] G. L. Yeo, C. A. Cornell, Post-quake decision analysis using dynamic programming, Earthquake Engineering & Structural Dynamics 38 (1) (2009) 79–93.

[13] G. L. Yeo, C. A. Cornell, Building life-cycle cost analysis due to mainshock and aftershock occurrences, Structural Safety 31 (5) (2009) 396 – 408.

[14] K. Helmut, Z. Mahmud, Cumulative damage in steel structures subjected to earthquake ground motions, Computers & Structures 16 (1) (1983) 531 – 541.

[15] E. DiPasquale, A. Cakmak, Seismic damage assessment using linear models, Soil Dynamics and Earthquake Engineering 9 (4) (1990) 194 – 215.

[16] E. DiPasquale, J. Ju, A. Askar, A. S. akmak, Relation between Global Damage Indices and Local Stiffness Degradation, Journal of Structural Engineering 116 (5) (1990) 1440–1456.

[17] L. Di Sarno, Evaluation of damage potential of recorded earthquake ground motion, Seismological Research Letters 72 (2001) 233.

[18] Y. Bozorgnia, V. V. Bertero, Improved shaking and damage parameters for post-earthquake applications, in: Proc., SMIP01 Seminar on Utilization of Strong-Motion Data, California Division of Mines and Geology, 1–22, 2001.

[19] J. Riascos-Ochoa, M. Sánchez-Silva, G.-A. Klutke, Modeling and reliability analysis of systems subject to multiple sources of degradation based on Lévy processes, Probabilistic Engineering Mechanics 45 (2016) 164–176.

[20] C. F. Choudhury, M. Ben-Akiva, M. Abou-Zeid, Dynamic latent plan models, Journal of Choice Modelling 3 (2) (2010) 50–70.

[21] T. Nakagawa, Shock and Damage Models in Reliability, Springer, London, 2007.

[22] U. Sumita, J. G. Shanthikumar, A Class of Correlated Cumulative Shock Models, Advances in Applied Probability 17 (2) (1983) 347–366.

[23] M. A. Wortman, G.-A. Klutke, H. Ayhan, A maintenance strategy for systems subjected to deterioration governed by random shocks., IEEE Transactions on Reliability 43 (3) (1994) 439–445.

[24] D. Montoro-Cazorla, R. Pérez-Ocón, A shock and wear system under environmental conditions subject to internal failures, repair, and replacement., Reliability Engineering and System Safety 99 (2012) 55–61.

[25] Y. J. Park, A. Ang, Mechanistic Seismic Damage Model for Reinforced Concrete, Journal of Structural Engineering ASCE 111 (4) (1985) 722–739.

[26] R. A. Hindi, R. G. Sexsmith, A Proposed Damage Model for RC Bridge Columns under Cyclic Loading, Earthquake Spectra 17 (2) (2001) 261–290.

[27] C. Michel, P. Gueguen, P. Y. Bard, Dynamic parameters of structures extracted from ambient vibration measurements: An aid for the seismic vulnerability assessment of existing buildings in moderate seismic hazard regions, Soil Dynamics and Earthquake Engineering 28 (8) (2008) 593–604.

[28] C. Aristizábal, P. Y. Bard, C. Beauval, J. Gómez, Integration of Site Effects into Probabilistic Seismic Hazard Assessment (PSHA): A Comparison between Two Fully Probabilistic Methods on the Euroseistest Site, Geosciences 8 (8) (2018) 285.

[29] D. M. Boore, Simulation of ground motion using the stochastic method, Pure and applied geophysics 160 (3-4) (2003) 635–676.

[30] G. Pousse, L. F. Bonilla, F. Cotton, L. Margerin, Nonstationary stochastic simulation of strong ground motion time histories including natural variability: Application to the K-net Japanese database, Bulletin of the Seismological Society of America 96 (6) (2006) 2103–2117.

[31] G. M. Atkinson, Earthquake time histories compatible with the 2005

National building code of Canada uniform hazard spectrum, Canadian Journal of Civil Engineering 36 (6) (2009) 991–1000.

[32] S. Rezaeian, A. Der Kiureghian, Simulation of synthetic ground motions for specified earthquake and site characteristics, Earthquake Engineering and Structural Dynamics 39 (10) (2010) 1155–1180.

[33] M. Marante, L. Suárez, L. Quero, J. Redondo, J. Vera, M. Uzcátegui, S. Delgado, L. León, L. Núñez, J. Flórez-López, Portal of damage: a web-based finite element program for the analysis of framed structrues subjected to overloads, Advances in Engineering Software 36 (5) (2005) 346–58.

[34] E. Sáez, F. Lopez-Caballero, A. Modaressi-Farahmand-Razavi, Inelastic dynamic soil-structure interaction effects on moment-resisting frame buildings, Engineering Structures 51 (1) (2013) 166–177.

[35] M. Giberson, Two nonlinear beams with definitions of ductility, Journal of Structural Division, ASCE 95 (2) (1969) 137–157.

[36] V. Prakash, G. Powel, S. Campbell, DRAIN 2D-X, Base program description and user guide, 1993.

[37] D. Aubry, A. Modaressi, GEFD*yn*, Manuel Scientifique, Ecole Centrale Paris, LMSS-Mat, 1996.

[38] K. Pitilakis, Z. Roumelioti, D. Raptakis, M. Manakou, K. Liakakis, A. Anastasiadis, D. Pitilakis, The EUROSEISTEST StrongMotion Database and Web Portal, Seismological Research Letters 84 (5) (2013) 796.

[39] A. Penna, S. Cattari, A. Galasco, S. Lagomarsino, Seismic Assessment of Masonry Structures by Non-linear Macro-element Analysis, in: IV International Seminar on Structural Analysis of Historical Construction-Possibilities of Numerical and Experimental Techniques, Padova, 1157–1164, 2004.

[40] C. Del Gaudio, M. T. De Risi, P. Ricci, G. M. Verderame, Empirical drift-fragility functions and loss estimation for infills in reinforced concrete frames under seismic loading, Bulletin of Earthquake Engineering 17 (3) (2019) 1285–1330.

[41] J. Woessner, D. Laurentiu, D. Giardini, H. Crowley, F. Cotton, G. Grünthal, G. Valensise, R. Arvidsson, R. Basili, M. B. Demircioglu, S. Hiemer, C. Meletti, R. W. Musson, A. N. Rovida, K. Sesetyan, M. Stucchi, The SHARE Consortium, The 2013 European Seismic Hazard Model: key components and results, Bulletin of Earthquake Engineering 13 (12) (2015) 3553–3596.

[42] D. M. Boore, Simulation of Ground Motion Using the Stochastic Method, pure and applied geophysics 160 (3) (2003) 635–676.

[43] D. M. Boore, SMSIM: Fortran Programs for Simulating Ground Motions from Earthquakes; version 2.3, Report a revision of OFR 96-80-A, U. S. Geological Survey; US Department of the Interior: Washington, DC, USA, 2005.

[44] W. B. Joyner, D. M. Boore, Peak horizontal acceleration and velocity from strong-motion records including records from the 1979 imperial

valley, California, earthquake, Bulletin of the Seismological Society of America 71 (6) (1981) 2011.

[45] G. D. Hatzigeorgiou, D. E. Beskos, Inelastic displacement ratios for SDOF structures subjected to repeated earthquakes, Engineering Structures 31 (11) (2009) 2744 – 2755.

[46] G. D. Hatzigeorgiou, A. A. Liolios, Nonlinear behaviour of RC frames under repeated strong ground motions, Soil Dynamics and Earthquake Engineering 30 (10) (2010) 1010 – 1025.

[47] J. Ruiz-Garca, J. C. Negrete-Manriquez, Evaluation of drift demands in existing steel frames under as-recorded far-field and near-fault mainshockaftershock seismic sequences, Engineering Structures 33 (2) (2011) 621 – 634.

[48] I. Iervolino, M. Giorgio, E. Chioccarelli, Closed-form aftershock reliability of damage-cumulating elastic-perfectly-plastic systems, Earthquake Engineering & Structural Dynamics 43 (4) (2014) 613–625.

[49] I. Iervolino, M. Giorgio, B. Polidoro, Reliability of structures to earthquake clusters, Bulletin of Earthquake Engineering 13 (4) (2015) 983–1002.

[50] S. Tesfamariam, K. Goda, G. Mondal, Seismic Vulnerability of Reinforced Concrete Frame with Unreinforced Masonry Infill Due to Main ShockAftershock Earthquake Sequences, Earthquake Spectra 31 (3) (2015) 1427–1449.

[51] F. Jalayer, H. Ebrahimian, Seismic risk assessment considering cumulative damage due to aftershocks, Earthquake Engineering & Structural Dynamics 46 (3) (2017) 369–389.

[52] M. R. Salami, M. M. Kashani, K. Goda, Influence of advanced structural modeling technique, mainshock-aftershock sequences, and ground-motion types on seismic fragility of low-rise RC structures, Soil Dynamics and Earthquake Engineering 117 (2019) 263 – 279.

[53] E. L. Kaplan, P. Meier, Nonparametric Estimation from Incomplete Observations, Journal of the American Statistical Association 53 (282) (1958) 457–481.